Published in final edited form as:
Macromolecules. 2013 February 12; 46(3): 1253–1259. doi:10.1021/ma3019975.

Synthesis of phenyleneethynylene-doped poly(pphenylenebutadiynylene) s for live cell imaging

Tereza Vokatá and **Joong Ho Moon***
Department of Chemistry & Biochemistry, Florida International University, Miami, Florida 33199, United States

Abstract

We developed a new synthetic approach to high molecular weight poly(p-phenylenebutadiynylene) s (PPBs) by increasing backbone flexibility. The introduction of a small amount of flexible units along the backbone improved both the physical and photophysical properties of the polymers. These materials were successfully fabricated into conjugated polymer nanoparticles (CPNs) and used for fluorescent live cell imaging for the first time.

INTRODUCTION

Conjugated polymers (CPs) are intrinsically fluorescent materials exhibiting the excellent photophysical properties (i.e., high brightness and photostability) necessary for various biological imaging,[1] sensing,[2] and delivery[3] applications. The high extinction coefficient, fluorescent quantum yields (QYs), and facile synthetic versatility of CPs make them promising materials for various biological applications. Recently, CPs with water-soluble side chains[4] and hydrophobic CPs blended with amphiphilic polymers have been used as immunofluorescence labels for live-cell imaging.[5] Protein detection has also been demonstrated with hybrid gold nanoparticle-CP conjugates.[6] Using weakly positively charged CPs, small interfering RNA (siRNA) delivery and target gene knockdown was also demonstrated.[3, 7]

Among CPs, poly(*p*-phenylenebutadiynylene)s (PPBs) are relatively less studied and used for biological applications, even though their synthesis is generally less sensitive to reaction environments. The resulting PPBs exhibit similar or better photophysical properties to their counterpart poly(*p*-phenyleneethynylenes) (PPEs).[8] PPB synthesis is commonly accomplished via the homo-coupling reaction between two terminal alkynes under Glaser or Hay coupling conditions,[9] as depicted in Scheme 1. Because the polymerization only involves alkyne monomers, there is no need for a precise stoichiometric balance to yield a high molecular weight polymer, which is a critical requirement for many step-polymerizations including the synthesis of PPEs and poly(*p*-phenylenevinylenes) (PPVs). Because of the similarity in the electronic properties of conjugated backbones, the absorption and emission profiles of both PPEs and PPBs are similar. However, PPBs are known to be less susceptible to oxidation due to the high oxidation potentials,[10] which contribute to their increased photostability under microscopic imaging conditions.

*Corresponding Author: jmoon@fiu.edu.

Author Contributions
The manuscript was written through contributions of both authors. All authors have given approval to the final version of the manuscript.

Supporting Information. ^{1}H NMR polymer spectra, FT-IR spectra, and CPN characterization. This material is available free of charge via the Internet at http://pubs.acs.org.

Despite the synthetic and photophysical advantages of PPBs, a limited number of PPB syntheses have been reported. Kijima et al. synthesized a series of PPBs and examined their semiconducting, fluorescence, and thermotropic liquid crystalline properties.[11] However, the PPBs exhibit low molecular weights (~5,000–9,000 g/mol) and poor solubility. Baier et al. prepared PPB nanoparticles in water using the miniemulsion polymerization technique.[12] While the authors reported that the molecular weight of the particles was ~20,000–40,000, such measurements may be overestimated due to chain aggregation within the nanoparticles. A common approach to increasing the solubility of CPs, as demonstrated in PPEs or PPVs, is the introduction of long and flexible side chains on the constituent monomers. However, the side chain modification is not enough to improve the solubility of PPBs, as the butadiyne units along the backbone provide an elongated structure prone to interpolymer interactions (i.e., interlocking). Williams et al. demonstrated various PPB syntheses with high molecular weights by the oxidative Sonogashira reaction of two alkynes with different side chains. In addition to the efficient oxidation of palladium by benzoquinone, the PPBs' randomness obtained from two alkynes is believed to improve the solubility and molecular weight of the block copolymers.[13] The same group also demonstrated that high molecular weight PPBs (up to ~124,000 g/mol) were synthesized by using bulky iptycene monomers, minimizing interchain stacking.[14] The rigid iptycene scaffolds are also known to minimize π-π stacking in solid films, preserving the photophysical properties suitable for ultrasensitive detection of chemicals.[15]

In this note, we report a new synthetic approach to achieving high molecular weight PPBs by increasing backbone flexibility. A series of deactivated aryl halides containing a flexible linker were synthesized and polymerized with an alkyne under the palladium/copper-mediated coupling conditions. High molecular weight PPBs (~38,000 g/mol) were successfully synthesized when the deactivated aryl bromide linker was reacted with an alkyne monomer. We found that the incorporation of a small amount (4–6%) of Sonogashira products [i.e., phenyleneethynylenes (PEs)] into the PPB backbone (i.e., PE-doped PPB, PE-d-PPB) is responsible for the improved physical and photophysical properties of PPBs. Finally, CPNs were fabricated by treating the PPB with organic acids followed by dialysis and used for fluorescent microscopic imaging of live cells.

EXPERIMENTAL SECTION

General

Chemicals, including solvents, were purchased from Fisher Scientific and used as received. *N-tert*-butoxycarbonyl (Boc)-protected cystine was purchased from Aldrich. Deuterated solvents were purchased from Cambridge Isotope Laboratories (Cambridge, MA). The average molecular weight (M_n) and polydispersity index (PDI = M_w/M_n) of the polymers were determined by gel permeation chromatography (GPC) against polystyrene standards using a Shimadzu high performance liquid chromatography (HPLC) system fitted with PLgel 5μm MIXED-D columns and SPD-20A ultraviolet-visible (UV-vis) detector. UV-vis spectra were recorded using a Varian Cary 50 Bio spectrophotometer. Fluorescence spectra were obtained using a FluoroLog-3 Spectrofluorometer (Jobin Yvon/Horiba). 9,10-diphenylanthracene (QY = 1.0) in cyclohexane was used as a fluorescence standard for QY determination. Fourier transform infrared (FT-IR) spectra were recorded on a PerkinElmer Spectrum 100 FT-IR Spectrometer. Fine polymer powders were directly mounted on an attenuated total reflection (ATR) cell of the spectrometer. Nuclear magnetic resonance (NMR) spectra were recorded on a 400 MHz Avance Bruker NMR spectrometer. Chemical shifts were reported in parts per million (ppm) for ^{1}H NMR on the δ scale based on the middle peak (δ = 2.50 ppm) of the dimethylsulfoxide (DMSO)-d_6 solvent as an internal standard. Dialysis and solvent exchange of CPNs were conducted using an Ultrafiltration Stirred Cell (Millipore) with membrane filters [Ultracel Ultrafiltration Disc, molecular

weight cut-off (MWCO): 30 kDa]. Hydrodynamic radii were determined by the dynamic light scattering technique using Zetasizer nano–ZS (Zen 3600, Malvern Instruments Ltd).

Synthesis of aryl halide linkers M2 and M3

Aryl bromide linker M2—Boc-protected cystine **1** (1.00 g, 2.27 mmol) was dissolved in anhydrous tetrahydrofuran (THF) (25 mL) in a round bottom flask, which was evacuated and filled with nitrogen. *N*-methylmorpholine (0.52 mL, 4.77 mmol) was added, and the suspension was allowed to stir until all the solid was dissolved. Isobutyl chloroformate (0.60 mL, 4.60 mmol) was added, and the mixture was allowed to stir at room temperature for 15 min. A solution of 4-bromoaniline (0.82 g, 4.77 mmol) in anhydrous THF (10 mL) was prepared under a N_2 atmosphere and transferred into the reaction flask using a cannula. The reaction was allowed to proceed for 3 h, after which the reaction mixture was filtered. The filtrate was concentrated *in vacuo,* and the resulting solid was washed with dichloromethane and precipitated overnight from the THF/ dichloromethane (DCM) solvent system. Yield: 0.50 g (29%). High-resolution mass spectrometry (MS) (ESI^+): theoretical 771.0316 m/z; experimental 771.0322 m/z [$M+Na^+$]. ^{1}H NMR (400 MHz, DMSO-d_6): δ 10.22 (s, 1H), 7.60 – 7.52 (m, 2H), 7.47 (d, J = 8.8 Hz, 2H), 7.25 (d, J = 7.9 Hz, 1H), 4.39 – 4.28 (m, 1H), 3.16 (dd, J = 13.3, 4.8 Hz, 1H), 3.00 – 2.89 (m, 1H), 1.37 (s, 9H). ^{13}C NMR (150 MHz): δ 169.3, 155.2, 138.1, 131.4, 121.4, 115.1, 78.4, 54.5, 28.1.

Aryl iodide linker M3—Following the procedure for the preparation of **M2**, the reaction between Boc-protected cystine **1** (0.50 g, 1.13 mmol) and 4-iodoaniline (0.52 g, 2.38 mmol) afforded the aryl iodide linker **M3**. Yield: 0.28 g (29%). High-resolution MS (ESI^+): theoretical 865.0058 m/z; experimental 865.0084 m/z [$M+Na^+$]. ^{1}H NMR (400 MHz, DMSO-d_6): δ 10.19 (s, 1H), 7.63 (d, J = 8.7 Hz, 2H), 7.43 (d, J = 8.8 Hz, 2H), 7.24 (d, J = 8.0 Hz, 1H), 4.33 (q, J = 8.0 Hz, 1H), 3.15 (dd, J = 13.3, 4.8 Hz, 1H), 3.01 – 2.89 (m, 1H), 1.37 (s, 9H). ^{13}C NMR (150 MHz): δ 169.3, 155.2, 138.5, 137.3, 121.7, 87.0, 78.4, 54.5, 28.1.

Polymer Synthesis

General procedure—A Schlenk flask was charged with monomer **M1** (or **M4**), monomer **M2** (or **M3**), $Pd[(PPh_3)_2Cl_2]$ (0.2 eq.) and CuI (0.95 eq). The Schlenk flask was evacuated and filled with N_2. A solution of anhydrous dimethylformamide (DMF) (4 mL) and freshly distilled triethylamine (1 mL) was degassed, and 1 mL of the mixed solution was transferred to the Schlenk flask via a cannula. The reaction was heated at 70°C for 14 h. The solution was then cooled to room temperature and transferred dropwise to cold ether, resulting in precipitation. After centrifugation (2 min, 4,000 rpm), the supernatant was decanted, and the precipitate was re-dissolved in DMF (1 mL) for further purification.

PPB_1: Using the general procedure described above, the polymerization of monomer **M1** (5.0 mg, 0.0111 mmol) in the presence of $Pd[(PPh_3)_2Cl_2]$ (1.6 mg, 0.00222 mmol) and CuI (2.0 mg, 0.0105 mmol) yielded PPB polymer **PPB_1** (3.2 mg, 64 %). ^{1}H NMR (400 MHz, DMSO-d6): δ 7.31 (s, 1H), 4.20 (br m, 2H), 3.76 (br m, 2H), 3.65-3.62 (m, 2H), 3.56-3.50 (m, 4H), 3.43-3.39 (m, 2H), 3.20 (s, 3H). FT-IR (neat): 3476, 2872, 2200, 1243, 1600, 1495, 1453, 1402, 1351, 1274, 1216, 1096, 1053, 944, 848, 722 cm^{-1}. GPC: M_w = 43,700 g/mol, M_n = 18,100 g/mol, PDI = 2.4. UV λ_{max} = 447 nm, Fluo λ_{max} = 479 nm, QY = 22%.

PPB_{1b}: Using the general procedure described above, the co-polymerization of monomer **M1** (5.0 mg, 0.0111 mmol) and 1,4-diethynylbenzene (1.4 mg, 0.0111 mmol) in the presence of $Pd[(PPh_3)_2Cl_2]$ (1.6 mg, 0.00222 mmol) and CuI (2.0 mg, 0.0105 mmol) yielded PPB co-polymer **PPB_{1b}** (1.5 mg, 23 %). Precipitation in the polymerization solution and poor solubility in DMF during the purification steps were responsible for the relatively poor

yield. ^{1}H NMR (400 MHz, DMSO-d6): δ 7.33 (s, 0.34H), 7.31 (s, 0.77H), 4.19 (br s, 2H), 3.77 (br s, 2H), 3.64-3.62 (m, 2H), 3.55-3.50 (m, 4H), 3.39 (m, 2H), 3.20 (s, 3H). FT-IR (neat): 2871, 2201, 1597, 1493, 1452, 1408, 1350, 1273, 1216, 1098, 1053, 940, 837, 720 cm^{-1}. GPC: M_w = 36,400 g/mol, M_n = 15,700 g/mol, PDI = 2.3. UV λ_{max} = 435 nm, Fluo λ_{max} = 474 nm, QY = 31%.

PPB$_2$: Using the general procedure described above, the polymerization of monomer **M1** (10.0 mg, 0.0222 mmol) and monomer **M2** (16.6 mg, 0.0222 mmol) in the presence of $Pd[(PPh_3)_2Cl_2]$ (3.1 mg, 0.00444 mmol) and CuI (4.0 mg, 0.0211 mmol) yielded the PE-d-PPB polymer **PPB$_2$** (8.9 mg, 78 %). ^{1}H NMR (400 MHz, DMSO-d6): δ 7.58 (d, 0.11H), 7.47 (d, 0.12H), 7.30 (s, 1H), 4.19 (br s, 2H), 3.76 (m, 2H), 3.63 (m, 2H), 3.54-3.51 (m, 4H), 3.40 (m, 2H), 3.20 (s, 3H), 1.37 (s, 0.57H). FT-IR (neat): 2872, 2203, 2142, 1693 cm^{-1} (carbamate C=O), 1592, 1495,1455, 1397, 1351, 1275, 1219, 1200, 1097, 1053, 946, 848, 633 cm^{-1}. GPC: M_w = 69,000 g/mol, M_n = 30,300 g/mol, PDI = 2.3. UV λ_{max} = 453 nm, Fluo λ_{max} = 478 nm, QY = 35%.

PPB$_3$: Using the general procedure described above, the polymerization of monomer **M4** (10.0 mg, 0.0188 mmol) and monomer **M3** (14.1 mg, 0.0188 mmol) in the presence of $Pd[(PPh_3)_2Cl_2]$ (2.6 mg, 0.00375 mmol) and CuI (3.4 mg, 0.0178 mmol) yielded Boc-protected amine PE-d-PPB polymer **PPB$_3$** (10.5 mg, 95 %). ^{1}H NMR (400 MHz, DMSO-d6): δ 7.57 (br m, 0.05H), 7.48 (br m, 0.07H), 7.30 (s, 1H), 6.73 (t, 1H), 4.18 (br s, 2H), 3.74 (br s, 2H), 3.49 (m, 2H), 3.11 (m, 2H), 1.35 (s, 9H). FT-IR (neat): 3343 (amide N-H), 2976, 2932, 2877, 2203, 1696 (carbamate C=O), 1494, 1455, 1391, 1364, 1272, 1248, 1219, 1165, 1123, 1054, 941, 779, 759 cm^{-1}. GPC: M_w = 75,900 g/mol, M_n = 34,000 g/mol, PDI = 2.2. UV λ_{max} = 456 nm, Fluo λ_{max} = 478 nm, QY = 25%.

PPE: Using the general procedure described above, the polymerization of monomer **M1** (5.0 mg, 0.0111 mmol) and monomer **M3** (9.4 mg, 0.0111 mmol) in the presence of $Pd[(PPh_3)_2Cl_2]$ (1.6 mg, 0.00222 mmol) and CuI (2.0 mg, 0.0105 mmol) yielded PPE polymer (8.8 mg, 75%). ^{1}H NMR (400 MHz, DMSO-d6): δ 10.32 (s, 1H, NH), 7.68 (d, 2H), 7.47 (d, 2H), 7.27-7.22 (m, 1H), 7.16 (s, 1H), 4.37 (br s, 1H), 4.16 (br s, 2H), 3.78 (br s, 2H), 3.66 (m, 2H), 3.51-3.46 (m, 4H), 3.38-3.28 (m, 2H), 3.18 (s, 3H), 3.10-2.92 (br m, 2H), 1.38 (s, 9H). FT-IR (neat): 3287 (amide N-H), 2984, 2939, 2874, 2208, 1689 cm^{-1} (carbamate C=O), 1591, 1516, 1493, 1406, 1365, 1311, 1278, 1245, 1216, 1199, 1160, 1097, 1050, 1021, 944, 837,775 cm^{-1}. GPC: M_w = 14,100 g/mol, M_n = 8,100 g/mol, PDI = 1.7. UV λ_{max} = 376 nm, Fluo λ_{max} = 408 nm and 445 nm, QY = 16%.

CPN formation

A solution of polymer **PPB$_3$** in DMSO-d_6 was mixed with acetic acid (2 mL) and trifluoroacetic acid (1 mL) and allowed to stir at room temperature for 14 days. The mixture was then added to acetic acid (20 mL), allowed to stir overnight, and centrifuged, and supernatant was added dropwise (2 drops/s) to 500 mL water (18 Ω) while stirring. Using a solvent-resistant stir cell fitted with a 30 kDa-MWCO membrane, the solution was concentrated to approximately 10 mL, and dialyzed against 1 L of water. The resulting solution was further dialyzed in a 10 KDa membrane for three days. The solution was subsequently filtered through a Teflon (PTFE) syringe filter (0.45 μm) and stored for future use. UV λ_{max} = 448 nm and 482 nm, Fluo λ_{max} = 532 nm (broad), QY = 0.5%.

Cell culture, microscopic imaging, and toxicity assay

~10,000 HeLa cells (human cervical cancer, purchased from ATCC) were seeded into a glass-bottomed eight-well chamber slide (Lab-Tek, Thermo Scientific) and cultured in a minimum essential medium (MEM) / Earle's balanced salt solution (EBSS) (400 μL,

HyClone, SH30024) medium containing 10% fetal bovine serum (FBS) and 100 U/m penicillin for 24 h under 5% CO_2 at 37°C. 80 μL of 20 μM CPNs in water was added to the culture medium directly, and the cells were further cultured for 24 h (final CPN concentration: 4 μM). For the golgi apparatus staining, BODIPY-TR C_5-ceramide-BSA complex (final 10 μM, Molecular probes, USA) was incubated for 30 min at 4°C. After washing with fresh medium, the cells were further incubated for 30 min at 37°C. 1 μL of Hoechst (5 μg/ml) was added to the culture medium and incubated with the cells for 10 min at 37°C, and washed two times with phosphate buffered saline (PBS). The cells were fixed with 4% paraformaldehyde for 10 min. Fluorescent images of the cells were obtained using a DeltaVision Elite Microscope System (Applied Precision, Issaquah, Washington) equipped with bandpass filters such as blue (410–460 nm, Hoechst) and green (500–550 nm, CPNs).

HeLa cells (~10,000 cells/well) in 200 μL of complete medium were seeded into a 96-well plate and cultured for one day in a 5 % CO_2 incubator at 37 °C. CPNs with various concentrations (5 to 40 μM) were added and incubated for 24 h. To measure toxicity, 10 μL of WST-1 [2-(4-Iodophenyl)-3-(4-nitrophenyl)-5-(2,4-disulfophenyl)-2H-tetrazolium] (CytoScan) solution was added into the each well, and the plate was further incubated for 4 h at 37 °C. Cell viability was compared by measuring absorbance values at 540 nm using a microplate well reader (Synergy 2, BioTek, USA). Relative cell viability as a function of CPN concentration was obtained by subtracting absorbance values of each sample well with control CPN absorbance at 540 nm.

RESULTS AND DISCUSSION

In order to improve the PPB backbone flexibility, the structure of the aryl halide linker necessitated the introduction of a flexible, non-conjugated moiety. Therefore, to synthesize the PE-d-PPB without compromising the characteristic photophysical properties of the fully conjugated PPB, we intended to incorporate only a minimal amount of the non-conjugated linker in the conjugated backbones. To accomplish this, we hypothesized that if the aryl halides are relatively inactive (i.e., electronically deactivated aryl bromides) under modified Sonogashira reaction conditions with high copper content, the alkyne homo-coupling will be predominant with a minor incorporation of Sonogashira reaction product.[16] This concept is the opposite of PPE synthesis, in which the cross coupling between alkynes and aryl halides is predominant, with minor incorporation of homo-coupling products.

Monomer Synthesis

To test our hypothesis, two aryl halides (**M2** and **M3**) were synthesized and reacted with an alkyne (**M1)** under conditions allowing both competing coupling reactions to occur. Both aryl halides were synthesized using a commercially available N-Boc-protected cystine, which was reacted with bromoaniline and iodoaniline to afford monomers **M2** and **M3**, respectively (Scheme 2). As the electron donating amide groups deactivate the $C_{sp}{}^2$-halide bonds of the aryl halides, the reactivity of the aryl bromide (**M2**) is expected to decrease significantly compared to that of the corresponding aryl iodide (**M3**). Under the high copper content in a typical Sonogashira reaction, the relatively inactive aryl bromides will not participate in the Sonogashira coupling cycles, allowing for the homo-coupling of alkynes to occur preferentially with a limited amount of Sonogashira coupling.

Polymer synthesis

A series of polymers was prepared under the palladium/copper catalytic conditions outlined in Scheme 3. To create a competing environment between the cross (i.e., Sonogashira) and homo (i.e., Glaser) coupling of the monomers, relatively high amounts of palladium [0.2 molar equivalent (eq)] and copper (0.9 eq) catalysts were used. The reaction was carried out

at 70°C overnight in a nitrogen environment. Physical and photophysical properties of the polymers were averaged using several independent batches of polymers and are summarized in Table 1. **PPB_1** synthesized by the homo-coupling of the monomer **M1** (in the absence of aryl halide) exhibit poor solubility in both DMF and DMSO and moderate molecular weights (number averaged molecular weight, M_n ~16 kg/mol) that can be achieved by other catalytic systems. When the aryl halides were reacted with **M1** under the same polymerization conditions, two different polymers (**PPE** and **PPB_2**) were obtained. While a PPB was obtained when the less reactive aryl bromide was used, polymerization with the aryl iodide led to the formation of a PPE. The chemical structure of **PPB_2** was assessed by ^{1}H NMR spectroscopy. As shown in Figure 1, **PPB_2** clearly contains the Boc group from linker **M2** at 1.37 ppm, and the integration ratio between the aromatic (from the PPB backbone) and Boc protons indicates that the incorporation of the flexible non-conjugating units was approximately 4–6%. The integration ratio also supported the formation of PPE when the **M1** monomer reacted with **M3**. The integration ratio between the aryl and Boc protons corresponds to the formation of 1:1 coupling between the two monomers (i.e., trimeric aryl conjugated units). When the more reactive aryl iodide (**M3**) was employed under the Sonogashira conditions, the oxidative addition of aryl iodide to Pd(0) was favorable (i.e., the reaction followed Sonogashira coupling cycles despite high copper concentration). Since the efficiency of the oxidative addition of aryl bromide to Pd(0) is relatively poor, Glaser coupling among copper coordinated-alkynes was observed when the deactivated aryl bromide (**M2**) was used. If the polymerization reaction contained an oxidant, the homo-coupling of two alkynes from Pd(II) could be possible, since the Pd(0) catalyst generated after the reductive elimination of butadiynes can be oxidized to Pd(II). Based on the polymerization results, we believe that Pd(0) was the active catalytic center for the cross-coupling reaction (i.e., PPE) and the homo-coupling reaction (i.e., PPB) occurred by the copper-mediated coupling reaction.

The absorption and emission spectra of PPE and PPBs were also representative (Figure 2). Since the PPE mainly contains trimeric conjugation units (confirmed by NMR analysis) due to the non-conjugating aryl iodides incorporated stoichiometrically along the chain, characteristic blue absorption from the trimers was observed. The presence of the shoulder at around ~425 nm indicates that the PPE may contain a small portion of butadiynylenes. Because the stoichiometric balance between **M1** and **M3** was broken by the homo-coupling of **M1**, the resulting PPE exhibits low molecular weight (M_n ~14K g/mol). However, when the less reactive aryl bromide **M2** was reacted with **M1** under the same conditions, completely different results were obtained. Even though an equivalent amount of the non-conjugating aryl bromide was used, the resulting polymer exhibits a red-shifted absorption (~450 nm) and emission (~478 nm), implying that the main backbones of the polymer are phenylenebutadiynylenes, and not phenyleneethynylenes.

The PPBs synthesized by the homo-coupling of an alkyne in the absence (i.e., **PPB_1**) or presence (**PPB_2**) of aryl bromides exhibit different physical and photophysical properties: **PPB_2** has higher molecular weight (38,000 g/mol), solubility in organic solvents, and QY than those of **PPB_1**.

FT-IR spectroscopy also provides evidence that **PPB_2** and **PPE** contain the carbonyl functional group found in the linker **M2**. The carbamate C=O stretch band, typically observed in the 1690-1630 cm^{-1} region, was clearly observed at 1689 cm^{-1} in the **PPE** FT-IR spectrum (Supporting Information). This band was absent in the case of the homo-polymer **PPB_1**. The FT-IR spectrum of **PPB_2** exhibited a shoulder at ~1692 cm^{-1} consistent with a low degree of **M2** linker incorporation (Supporting Information).

High molecular weights, solubility, and QYs were consistently obtained only when the aryl bromide was used for the polymerization reaction. To confirm the flexibility effects on the physical properties, we co-polymerized monomer **M1** with 1,4-diethynylbenzene, which lacks the flexible moiety of the linker **M2** but mimics its aromatic group (Scheme 4). Similar to the conventional PPB (i.e., $\mathbf{PPB_1}$ that was synthesized in the absence of the linker), the reaction solution produced insoluble materials, and the resulting polymer exhibited poor solubility in DMF during the purification processes. The soluble fraction of the resulting polymer $\mathbf{PPB_{1b}}$ exhibited molecular weight similar to that of the homo-polymer $\mathbf{PPB_1}$, and its ^{1}H NMR spectrum showed approximately 22% 1,4-diethynylbenzene incorporation (Supporting Information). We therefore conclude that the incorporation of a small quantity of non-conjugating but flexible PE units in the polymer backbone (i.e., **M2** doping) increases the flexibility of the resulting PPBs and decreases interchain aggregations, resulting in high molecular weight PPBs with preserved photophysical properties.

Decreasing the relative amount of monomer **M2** (0.2 eq) compared to **M1** in the polymerization produces PE-d-PPBs with a reduced PE incorporation ($\mathbf{PPB_{2a}}$, percent incorporation could not be determined due to low signals), while an excess amount of **M2** (2.0 eq) did not proportionally increase the incorporation ratio in the PE-d-PPB ($\mathbf{PPB_{2c}}$). Based on these observations, we conclude that in order to achieve the desired PE doping effect during polymerization, the deactivated aryl bromide flexible linker must have at least an equimolar concentration.

Cellular imaging

Since the cellular membranes contain negatively charged proteoglycans and hydrophobic lipid bilayers, weakly positively charged hydrophobic CPNs exhibit high interaction with the membranes[17] and subsequent cellular entries through various endocytosis pathways.[18] Unlike polymers containing quaternized ammonium salts, which cause cellular toxicity, primary amine-containing CPNs exhibit no cellular toxicity owing to the low charge-to-molecular weight ratio (i.e., 1/43 and 1/255 for polyethyleneimine and CPN, respectively).[19]

To apply the PE-d-PPBs for live cell imaging, we polymerized a Boc-protected amine-containing alkyne **M4** in the presence of the aryl bromide **M2** (Scheme 2). The resulting amine-containing PE-d-PPB $\mathbf{PPB_3}$ exhibits similar physical and photophysical properties to those of PE-d-PPB $\mathbf{PPB_2}$ (Table 1). After deprotection of the Boc groups upon treatment with trifluoroacetic acid, CPNs were fabricated by dialysis as described previously.[20] The CPNs exhibited a hydrodynamic radius of ~50 nm with a broad size distribution (Supporting Information).

The metabolic activities of HeLa cells incubated with CPNs were monitored using WST-1 assay. Succinate-tetrazolium reductases in viable cells reduce tetrazolium salts to colored (540 nm) formazan, and the viability inhibition can be assessed by comparing formazan concentrations between control (no treatment) and sample (CPN treated) cells. As shown in Figure 3, formazan production from the cells treated with CPNs was similar to the control cells, indicating that CPNs exhibit no viability inhibition under the treatment condition.

CPNs were accumulated in cytosolic compartments shown as green dots [Figure 4(b)], not in the nucleus. To identify the subcellular localization of CPNs, we co-stained the CPN-containing HeLa cells with a golgi-specific fluorescent probe [red, BODIPY-TR C_5-ceramide-bovine serum albumin (BSA) complex]. As shown in Figure 4(d), high overlaps (yellow or orange dots) between CPNs and BODIPY-TR C_5-ceramide-BSA complex were observed, implying that CPNs were trafficked by an endocytosis mechanism (i.e., caveolae-mediated endocytosis[21]) to the golgi appratus.

CONCLUSION

In conclusion, we have developed a new synthetic method to improve the physical and photophysical properties of PPBs by increasing the flexibility of the polymer backbone. The incorporation of a small quantity of non-conjugating, flexible units in the PPB backbone leads to the successful synthesis of high molecular weight PE-d-PPBs (~38,000 g/mol). We also demonstrated that PE-d-PPBs are useful materials for fluorescent live cell imaging. The newly developed doping technique is well suited for the synthesis of polar side chain-containing PPBs, showing promise for future use in biological sensing and labeling.

Supplementary Material

Refer to Web version on PubMed Central for supplementary material.

Acknowledgments

Funding Sources

National Institutes of Health (NIH)

This work was supported by NIH/NIGMS SC1 (grant #: GM092778).

References

1. (a) Moon JH, McDaniel W, MacLean P, Hancock LF. Angew Chem Int Ed. 2007; 46:8223–8225.(b) Rahim NAA, McDaniel W, Bardon K, Srinivasan S, Vickerman V, So PTC, Moon JH. Adv Mater. 2009; 21:3492–3496.(c) Kim IB, Shin H, Garcia AJ, Bunz UHF. Bioconjugate Chem. 2007; 18:815–820.
2. (a) Chen L, McBranch DW, Wang HL, Helgeson R, Wudl F, Whitten DG. Proc Natl Acad Sci USA. 1999; 96:12287–12292. [PubMed: 10535914] (b) Disney MD, Zheng J, Swager TM, Seeberger PH. J Am Chem Soc. 2004; 126:13343–13346. [PubMed: 15479090] (c) Feng F, He F, An L, Wang S, Li Y, Zhu D. Adv Mater. 2008; 20:2959–2964.(d) Gaylord BS, Heeger AJ, Bazan GC. J Am Chem Soc. 2003; 125:896–900. [PubMed: 12537486] (e) Ho HA, Boissinot M, Bergeron MG, Corbeil G, Doré K, Boudreau D, Leclerc M. Angew Chem Int Ed. 2002; 41:1548–1551.(f) Kim IB, Wilson JN, Bunz UHF. Chem Commun. 2005; 41:1273–1275.(g) Pu KY, Liu B. Adv Funct Mater. 2009; 19:277–284.(h) Wosnick JH, Mello CM, Swager TM. J Am Chem Soc. 2005; 127:3400–3405. [PubMed: 15755158]
3. Moon JH, Mendez E, Kim Y, Kaur A. Chem Commun. 2011; 47:8370–8372.
4. (a) Lee K, Lee J, Jeong EJ, Kronk A, Elenitoba-Johnson KSJ, Lim MS, Kim J. Adv Mater. 2012; 24:2479–2484. [PubMed: 22488758] (b) Kim HJ, Lee J, Kim TH, Lee TS, Kim J. Adv Mater. 2008; 20:1117–1121.
5. (a) Wu C, Schneider T, Zeigler M, Yu J, Schiro PG, Burnham DR, McNeill JD, Chiu DT. J Am Chem Soc. 2010; 132:15410–15417. [PubMed: 20929226] (b) Yu JB, Wu CF, Zhang XJ, Ye FM, Gallina ME, Rong Y, Wu IC, Sun W, Chan YH, Chiu DT. Adv Mater. 2012; 24:3498–3504. [PubMed: 22684783]
6. You CC, Miranda OR, Gider B, Ghosh PS, Kim IB, Erdogan B, Krovi SA, Bunz UH, Rotello VM. Nat Nanotechnol. 2007; 2:318–323. [PubMed: 18654291]
7. Silva AT, Alien N, Ye CM, Verchot J, Moon JH. BMC Plant Biol. 2010; 10:291. [PubMed: 21192827]
8. (a) Bunz UHF. Chem Rev. 2000; 100:1605–1644. [PubMed: 11749277] (b) Bunz UHF. Macromol Rapid Commun. 2009; 30:772–805. [PubMed: 21706662]
9. Mundy, BP.; Ellerd, MG.; Favaloro, FG, Jr. Name Reactions and Reagents in Organic Synthesis. 2. Wiley-Interscience; New Jersey: 2005. p. 276

10. (a) Egbe DAM, Birckner E, Klemm E. J Polym Sci, Part A: Polym Chem. 2002; 40:2670–2679.(b) Egbe DAM, Carbonnier B, Paul EL, Muhlbacher D, Kietzke T, Birckner E, Neher D, Grummt UW, Pakula T. Macromolecules. 2005; 38:6269–6275.
11. (a) Kijima M, Kinoshita I, Hattori T, Shirakawa H. J Mater Chem. 1998; 8:2165–2166.(b) Kijima M, Kinoshita I, Hattori T, Shirakawa H. Synth Met. 1999; 100:61–69.
12. Baier MC, Huber J, Mecking S. J Am Chem Soc. 2009; 131:14267–14273. [PubMed: 19764722]
13. Williams VE, Swager TM. J Polym Sci, Part A: Polym Chem. 2000; 38:4669–4676.
14. Zhao D, Swager TM. Macromolecules. 2005; 38:9377–9384.
15. Yang JS, Swager TM. J Am Chem Soc. 1998; 120:5321–5322.
16. (a) Chinchilla R, Najera C. Chem Rev. 2007; 38:874–922. [PubMed: 17305399] (b) Schilz M, Plenio H. J Org Chem. 2012; 77:2798–2807. [PubMed: 22390837]
17. Tan SJ, Jana NR, Gao SJ, Patra PK, Ying JY. Chem Mater. 2010; 22:2239–2247.
18. Duncan R, Richardson SCW. Mol Pharm. 2012; 9:2380–2402. [PubMed: 22844998]
19. Lee Y, Mo H, Koo H, Park JY, Cho MY, Jin GW, Park JS. Bioconjugate Chem. 2007; 18:13–18.
20. Ko YJ, Mendez E, Moon JH. Macromolecules. 2011; 44:5527–5530. [PubMed: 21808426]
21. Sahay G, Kim JO, Kabanov AV, Bronich TK. Biomaterials. 2010; 31:923–933. [PubMed: 19853293]

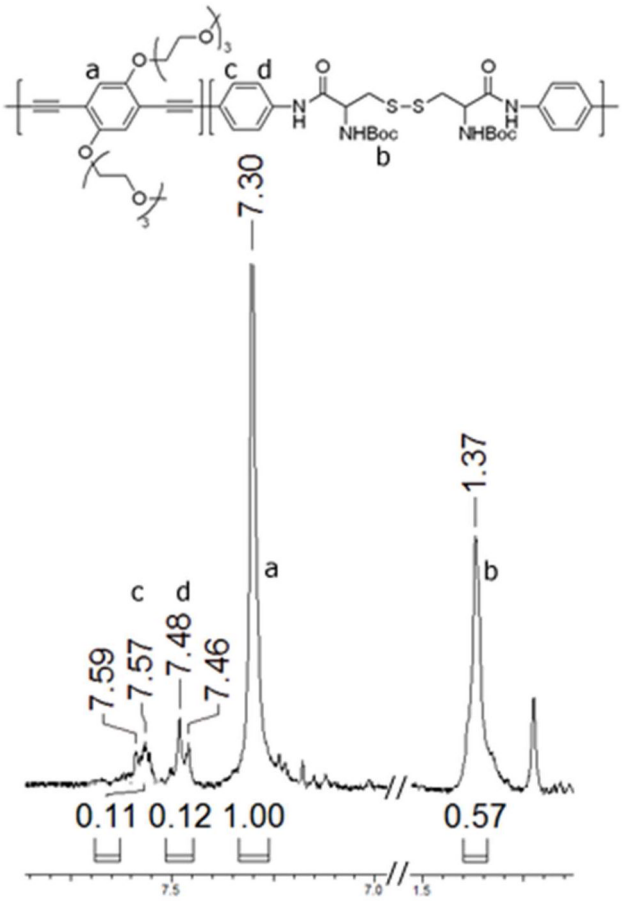

Figure 1.
Illustration of the ^{1}H NMR determination of the percent incorporation of monomer **M2** into the PPB polymer backbone.

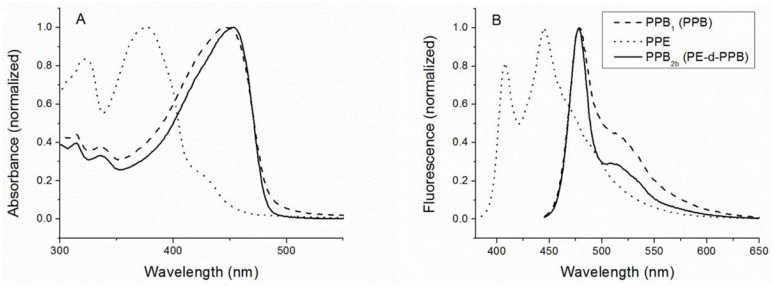

Figure 2.
Normalized absorption (A) and emission (B) spectra of polymers **PPB_1**, **PPB_{2b}**, and **PPE** in DMF.

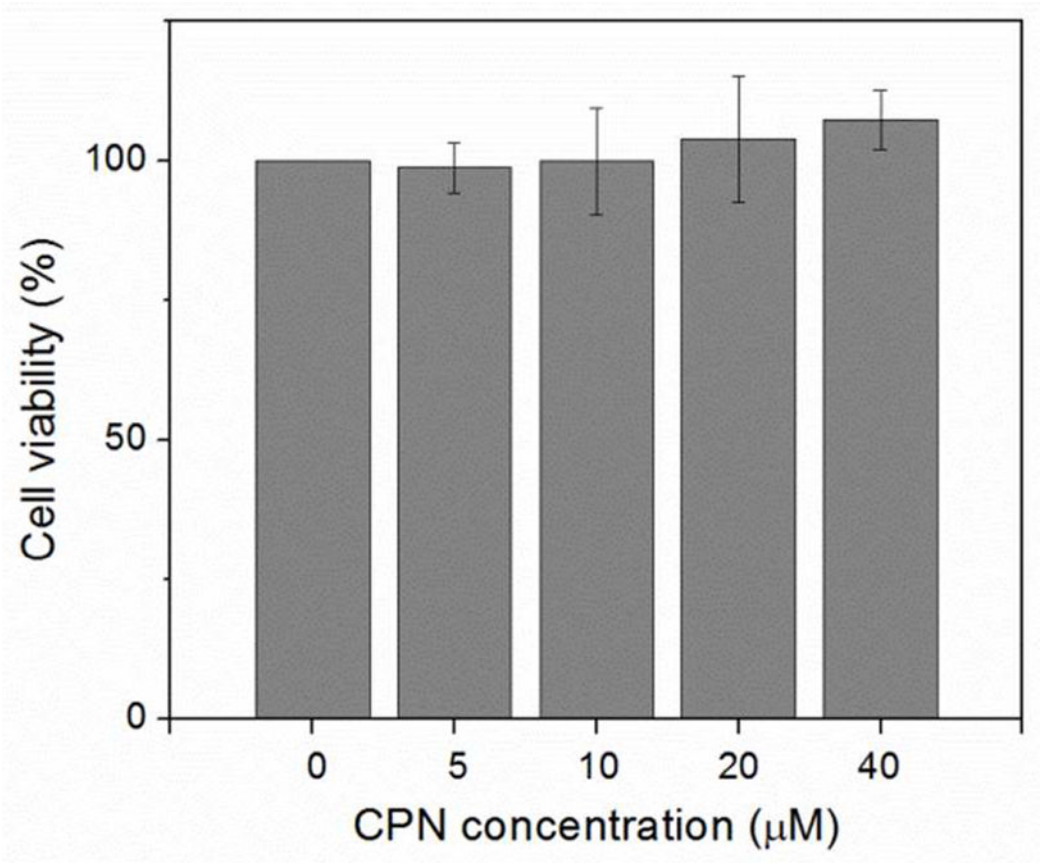

Figure 3.
Cell viability evaluation by WST-1 assay. CPNs cause no viability inhibition.

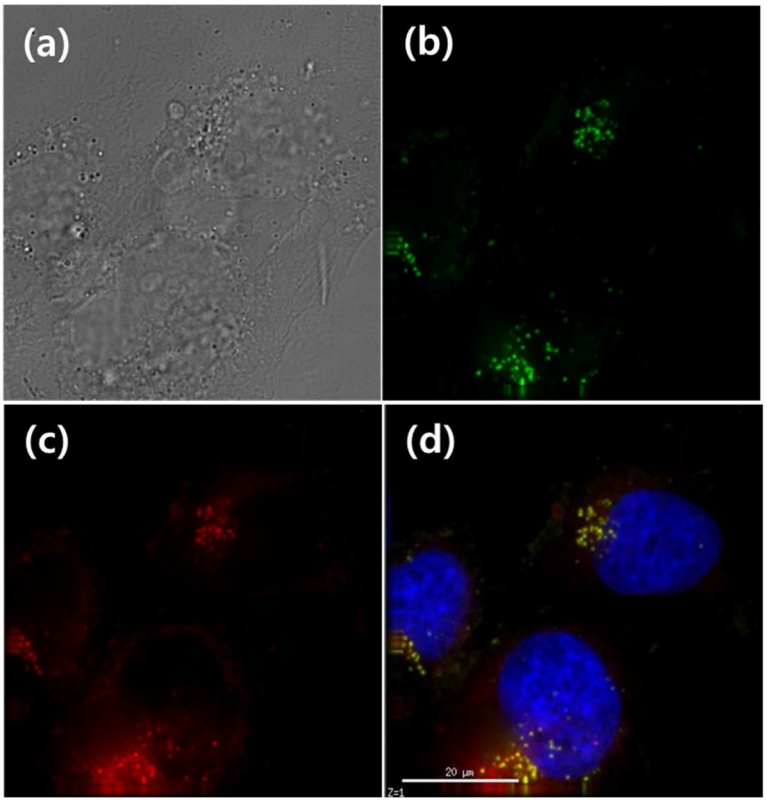

Figure 4.
Microscopic images of HeLa cells incubated with **PPB_3** CPNs. Green fluorescent CPNs (b) were accumulated in the golgi apparatus (c), confirmed by overlapped signals (yellow) in the composed image (d). A contrast image is shown in (a).

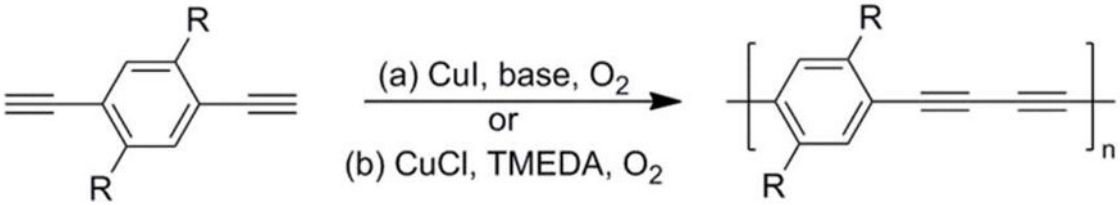

Scheme 1.
Formation of PPB under (a) Glaser and (b) Hay coupling conditions.

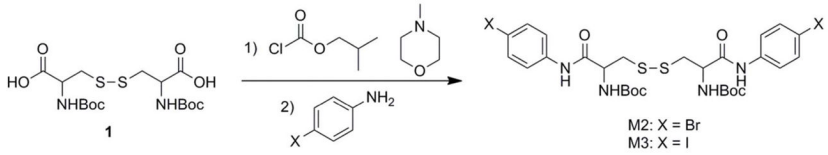

Scheme 2.
Synthesis of aryl halide monomers **M2** and **M3**.

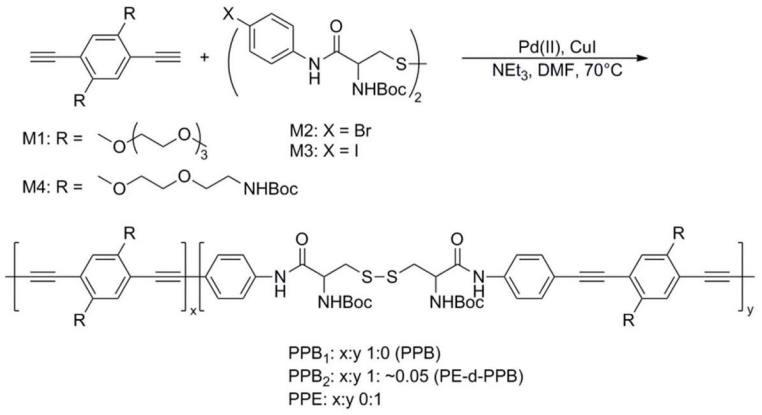

Scheme 3.
Synthesis of PPB_1, PE-d-PPB, and PPE.

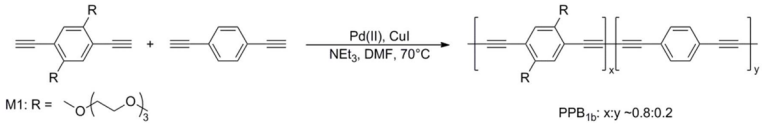

Scheme 4.
Synthesis of PPB co-polymer **PPB_{1b}**.

Table 1

Comparison of the average physical and photophysical properties of PPE, PPB, and PE-d-PPBs.

Polymer	Type	M1:M2 ratio	M_w (g/mol)[a]	M_n (g/mol)[a]	PDI[b]	$\lambda_{max, abs}$ (nm)[c]	$\lambda_{max, em}$ (nm)[c,d]	QY (%)[e]	M2 monomer incorporation (%)[f]
PPB_1	PPB	1: 0	37,400	16,600	2.3	447	479	17	-
PPB_{2a}	PE-d-PPB	1: 0.2	23,400	11,200	2.1	434	477	9	n.d.
PPB_{2b}	PE-d-PPB	1: 1	97,400	38,400	2.5	453	478	32	6
PPB_{2c}	PE-d-PPB	1: 2	97,900	40,100	2.4	453	478	34	4
PPB_3	PE-d-PPB	1: 1 [h]	71,100	32,400	2.2	455	478	31	-
PPE	PPE	1: 1 [i]	14,100	8,100	1.7	376	408/445	16	-

[a] Determined by gel permeation chromatography in THF.

[b] PDI (polydispersity index) = M_W/M_n.

[c] Measured in DMF.

[d] PPB_1 and PPB_2 excitation wavelength 430 nm, PPE excitation wavelength 370 nm in DMF.

[e] Quantum yield in DMF measured relative to diphenylanthracene standard.

[f] Determined by ^{1}H NMR peak integration.

[g] Not determined due to low signal to noise ratio of the ^{1}H NMR signals.

[h] M4:M2 ratio 1:1.

[i] M1:M3 ratio 1:1.